Reexamination of Refrigeration Power of the LHD Cryogenic System After Fire and Restart of Operation

Toshiyuki Mito, Akifumi Iwamoto, Shinji Hamaguchi, Sadatomo Moriuchi, Koki Oba, Shigeyuki Takami, Hiroki Noguchi, Kazuya Takahata, Nagato Yanagi, Shinsaku Imagawa, Takuya Kumaki, Koji Obara, Minoru Nobutoki, Katsuhiro Nakamura, Toshiya Nakashima, and Shigeharu Kuwahara

***Abstract*—The Large Helical Device (LHD), built in the 1990s, is a heliotron-type fusion plasma experimental device with the world's first fully superconducting magnetic confinement system. The LHD cryogenic system operated stably for 18 years from 1998 to 2015 with high availability exceeding 99%. Unfortunately, in August 2015, a fire occurred in the cold box of the He refrigerator during maintenance, and nonmetallic components such as multilayer insulation films, temperature sensors, and measuring instruments were burnt down. Repair work started in November 2015 and completed at the end of July 2016. In August 2016, a test operation of the He refrigerator was conducted, and the refrigeration power was compared with that measured in the initial performance test conducted in 1995. The measured equivalent refrigeration power at 4.4 K was 9.19 kW, representing a decrease ∼2% from the value of 9.38 kW measured in 1995. We attributed this slight decrease in refrigeration power to performance deterioration owing to aging over 18 years and not to the fire. The LHD restarted operation in January 2017, and its 19th operational cycle for a deuterium plasma experiment was conducted successfully up to August 2017. This paper reports the operational history and restart of the LHD superconducting magnet and cryogenic system.**

***Index Terms*—Cryogenic system, fusion plasma, Large Helical Device (LHD), magnetic confinement, operational history.**

I. Introduction

THE Large Helical Device (LHD) is a heliotron-type fusion plasma experimental machine that can confine currentless, high-density, and high-temperature plasmas in a steady state. The steady magnetic field at the plasma center is 3 T. The LHD has a fully superconducting magnet system consisting of helical coils, poloidal coils, and superconducting bus-lines cooled by a He refrigerator with total equivalent cooling capacity of 9.2 kW at 4.4 K. The LHD superconducting coils are installed in the cryostat. The LHD cryostat has outer diameter and height of 13.5 m and 8.8 m, respectively, and its total weight is 1,500 tons. The cold mass at 4.4 K in the cryostat weighs 820 tons. Three different cooling schemes are used: forced flow of supercritical He for the poloidal coils, forced flow of two-phase He for the supporting structure for the large electromagnetic forces between the superconducting coils, and pool boiling of liquid He for the helical coils. The LHD superconducting coils were excited using nine superconducting bus-lines with total length of 497 m and maximum current capacity of 31.3 kA each. The bus-lines are also cooled by the forced flow of two-phase He. Fig. 1 shows the components of the LHD superconducting and cryogenic system [1]–[4].

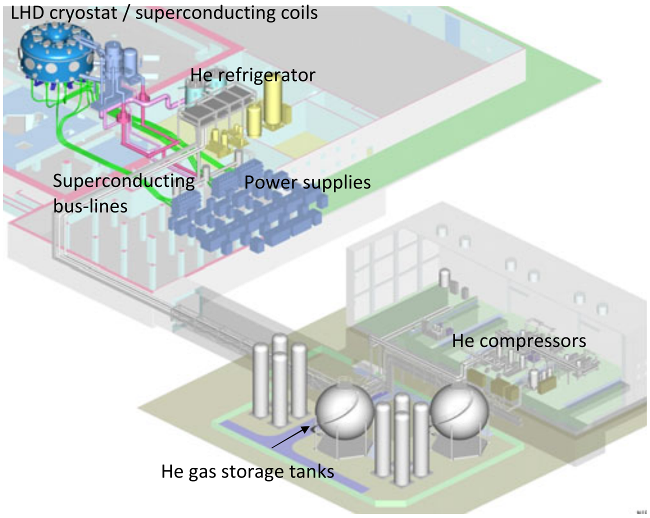

Fig. 1. Layout of the LHD superconducting and cryogenic system.

II. Repair of the He Refrigerator

A. Fire in the He Refrigerator

The LHD cryogenic system had been operated stably for 18 years from 1998 to 2015 with high availability exceeding 99% [5]. Then, in August 2015, a fire occurred in the cold box of the He refrigerator during maintenance. Fig. 2 shows the equipment layout in the He refrigerator room.

Manuscript received September 19, 2017; accepted February 5, 2018. Date of publication February 28, 2018; date of current version May 17, 2018. This work was supported by the National Institute for Fusion Science (ULAA701/704). *(Corresponding author: Toshiyuki Mito.)*

T. Mito, A. Iwamoto, S. Hamaguchi, S. Moriuchi, K. Oba, S. Takami, H. Noguchi, K. Takahata, N. Yanagi, and S. Imagawa are with the National Institute for Fusion Science, National Institutes of Natural Sciences, Toki 509-5292, Japan (e-mail: mito@nifs.ac.jp; iwamoto@LHD.nifs.ac.jp; hamaguchi@LHD.nifs.ac.jp; moriuchi@LHD.nifs.ac.jp; ooba@LHD.nifs.ac.jp; takami@LHD.nifs.ac.jp; noguchi@LHD.nifs.ac.jp; takahata@LHD.nifs.ac.hp; yanagi@LHD.nifs.ac.jp; imagawa@LHD.nifs.ac.jp).

T. Kumaki, K. Obara, M. Nobutoki, K. Nakamura, T. Nakashima, and S. Kuwahara are with the Taiyo Nippon Sanso Corporation, Kawasaki 210-0861, Japan (e-mail: Takuya.Kumaki@tn-sanso.co.jp; Koji.Obara@tn-sanso.co.jp; Katsuhiro.Nakamura@tn-sanso.co.jp; Toshiya.Nakashima@tn-sanso.co.jp; Shigeharu.Kuwahara@tn-sanso.co.jp).

Color versions of one or more of the figures in this paper are available online at http://ieeexplore.ieee.org.

Digital Object Identifier 10.1109/TASC.2018.2810517

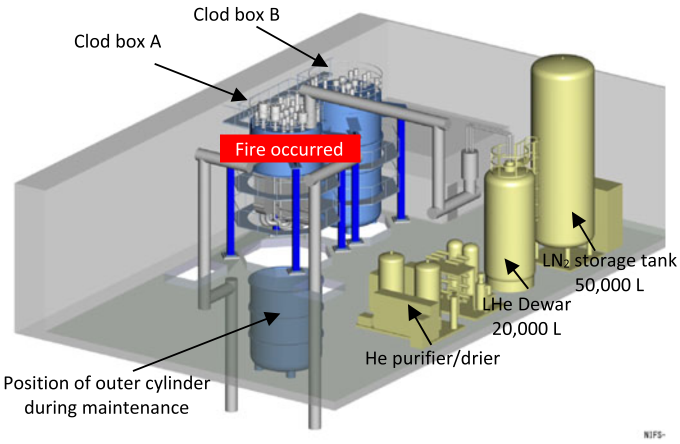

Fig. 2. Equipment layout in the He refrigerator room.

The He refrigerator consists of two cold boxes, one each for the high-temperature side (cold box B) and low-temperature side (cold box A), a 20,000-L liquid He (LHe) Dewar, a 50,000-L liquid N_2 storage tank, and a 50 g/s He gas purifier/drier. Both cold boxes are covered by an outer cylinder during operation and are kept in a vacuum state. In the 18th operational cycle, a differential pressure rise was observed at the turbine inlet filters; this was caused by accumulated contamination during long-term operation. Then, the turbine filters and internal absorbers (ADS-1) were replaced during maintenance after the 18th operational cycle. Fig. 2 shows the outer cylinder of cold box A taken down during maintenance while cold box B was still operating. The fire occurred when welding a replacement fourth turbine inlet filter in cold box A. The nonmetallic components in cold boxes A and B, such as multilayer insulation films, temperature sensors, and measuring instruments, were burnt down.

Fig. 3 shows the configuration of cold boxes A and B. The He refrigerator consists of seven expansion turbines (T1–T7) with dynamic gas bearing and 15 heat exchangers (HX-1–HX-15). The nominal cooling capacities are 5.65 kW at 4.4 K and 20.6 kW for 40–80 K, and the liquefaction rate is 650 L/h for the current leads.

After the accident, the repair work started in November 2015, and it was completed at the end of July 2016. The repairs that were conducted are listed below.

- Cleaning of building and installation equipment in He refrigerator room
- Cleaning inside the cold box
- Restoration of cold box functionality
  - Check and cleaning of inner surface of piping in the cold box
  - Connection of piping for turbine inlet filters and ADS-1
  - Check of control valves/manual valves
  - He leakage test
  - Check of integrity of piping/heat exchangers
  - Inspection of piping construction part (the completion test for the High-Pressure Gas Safety Act retooling application was included)
  - Replacement of 86 temperature sensors (including dual redundant sensors and interlock sensors) in the cold box
  - Repair of power wiring for heaters and external wiring for sensors
  - Installation of multilayer insulation films
  - Vacuum substitution with He gas in piping system
  - He gas purification in the cold box
  - Overhaul of ADS-1 exit valve
  - Installation of seven turbines

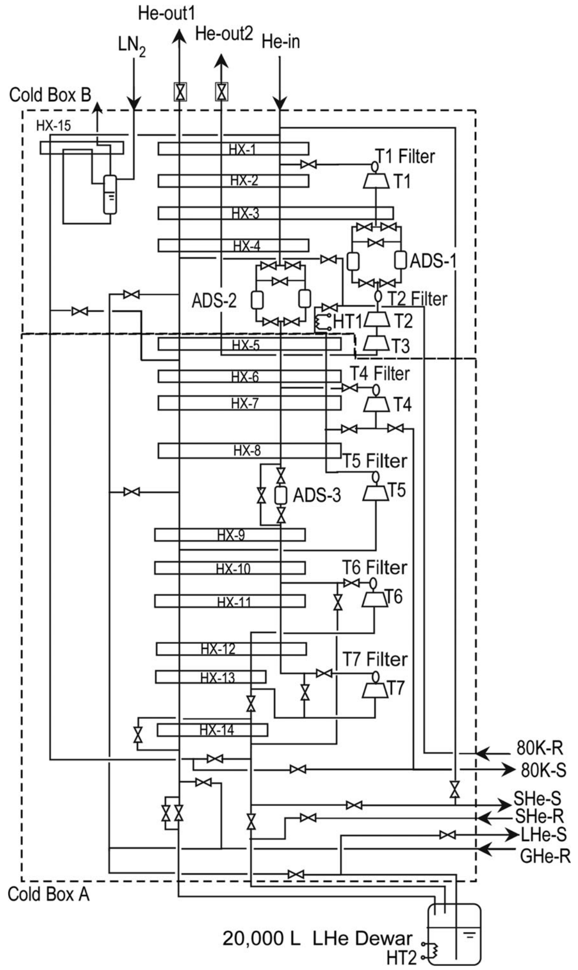

Fig. 3. Configuration of cold boxes A and B of the He refrigerator.

B. Test Operation of the He Refrigerator

After the repair work, a test operation of the He refrigerator was conducted in August 2016. The control characteristics of the replacement temperature sensors and performance characteristics of the control valves were confirmed simultaneously. The test operations were scheduled as follows.

August 1: Preliminary work before test operation

- Backup and modification of automatic control program for individual operation of He refrigerator
- Separation of He refrigerator from the LHD superconducting system
- Check of valve opening and closing positions
- Installation of power meters for power supplies of heaters

August 2: Start of test operation

- Startup of He compressors

TABLE I
COMPARISON OF MEASURED REFRIGERATION POWER

Refrigeration power	Measurement on August 5, 2016	Measurement on June 17, 1995
4.4 K refrigeration power (measured by heater input of HT2 in LHe Dewar)	5.67 kW	5.67 kW
4.4 K liquefaction ability (measured by LHe level sensor in LHe Dewar)	606 L/h	704 L/h
80 K refrigeration power (measured by heater input of HT1 at 80 K)	23.35 kW	20.7 kW
4.4 K equivalent refrigeration power	9.19 kW	9.38 kW

- Purification of He gas in the He refrigerator and check of gas purity and dew point

August 3: Start of precooling stage

- Startup of turbines 1–5

August 4: Start of refrigeration stage

- Startup of turbines 6–7

August 5: Measurement of refrigeration power

- The heater power of HT2 corresponding to the refrigeration heat loads was input at 4.4 K (5.67 kW) and the heater power of HT1 was input to keep the outlet temperature at 80 K (23.35 kW or 20.7 kW), and the He liquefaction capacity was measured using the liquid He level meter in the 20,000-L LHe Dewar.
- Confirmation of the accuracy of the replaced thermometers in the cold box

August 6–7: Warm-up operation

August 8: End of test operation

- Shutdown of He compressors and end treatment for shutdown

During typical LHD operation, one month each is needed for the warm-up and cool-down of the LHD superconducting system. However, the refrigeration power could be confirmed through one-week operation of the He refrigerator without the LHD superconducting system.

C. Reexamination of Measured Refrigeration Power

The measured refrigeration power was compared with that measured in the initial performance test conducted in June 1995, as shown in Table I. The refrigeration power at 4.4 K was measured as the input power to heater HT2 in the LHe Dewar. The He liquefaction ability at 4.4 K was measured from the rate of increase seen in the LHe level sensor in the LHe Dewar. The refrigerating power at 80 K was measured as the input power to heater HT1 that was set up between outlet T4 and inlet T5. Heater HT1 was controlled using the LTIC2013 controller such that the He gas temperature at the heater outlet became 80 K. An equivalent refrigeration power was obtained based on the three above mentioned measurements, and it was converted into the refrigeration power at 4.4 K. The measured equivalent refrigeration power at 4.4 K in 2016 was 9.19 kW; this represented a decrease of $\sim$2% from the measured value of 9.38 kW in 1995. We attribute this slight decrease in refrigeration power to performance deterioration owing to aging and problems such as dirt in the heat exchangers over 18 years operation, and not to the direct influence of the fire. In the computer simulation results, the decrease in refrigeration power can be explained by assuming that the heat transfer length of heat exchangers EX1–EX4 decreased from 100% to 87% owing to factors such as oil adhering to the heat exchanger surface.

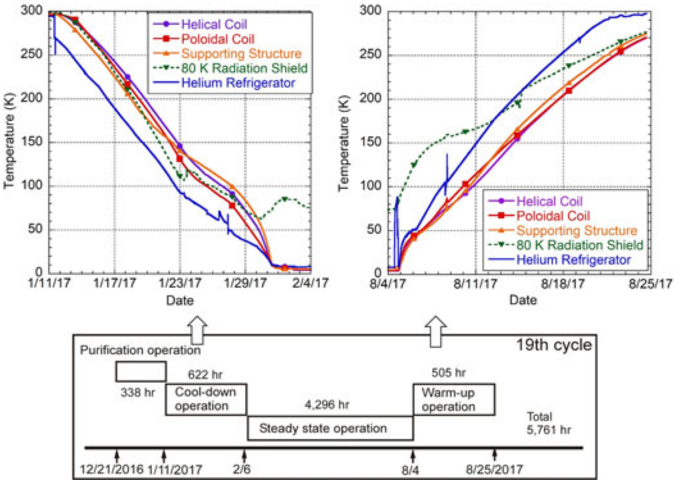

Fig. 4. Nineteenth operational cycle of the LHD cryogenic system.

At 34 measurement points with the replaced temperature sensors, problematic measurement differences were not observed. The control valves can be operated more stably by improving the software and hardware relative to that used at the start of operations in 1995. The degradation of the LHD cryogenic system can be minimized through appropriate maintenance, and its performance has been well maintained despite 18 years of operation. The operation tests confirmed that the 19th operational cycle of the LHD for deuterium experiments could be started.

III. NINETEENTH OPERATIONAL CYCLE OF LHD

A. Nineteenth Operational Cycle of the LHD Cryogenic System

Fig. 4 shows the 19th operational cycle of the LHD cryogenic system. The compressors of the LHD cryogenic system were started on December 21, 2016. A 338-h purification operation was performed to reduce the impurity contamination in the He cryogenic system below 1 ppm before the end of the year. Then, the LHD superconducting system was allowed to cool down for 622 h such that the temperature gradient in the system reduced below 50 K. Steady-state operation of the LHD in the superconducting state was conducted for 4,296 h from February 6 to August 4, 2017.

On March 7, 2017, the deuterium experiment in which the plasma-generating gas was changed from hydrogen into deuterium was started. A plasma ion temperature of 120 million

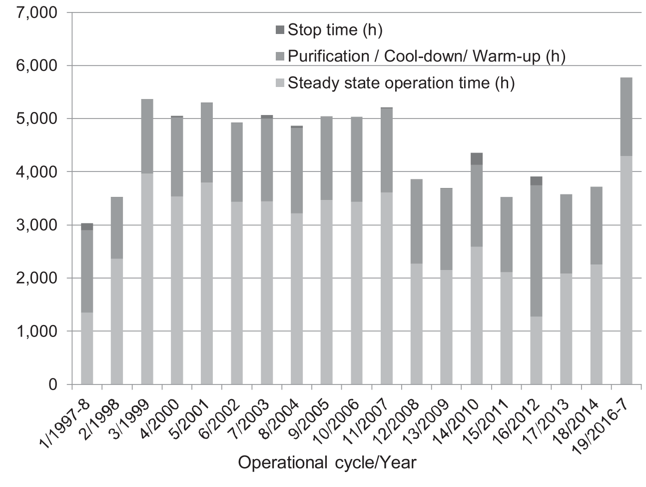

Fig. 5. Operational history of the LHD cryogenic system.

degrees was achieved in this experiment. This temperature was one of the most important plasma conditions, and it established the feasibility to the helical-type fusion reactor.

The He compressors did not stop during the steady-state operation. However, the brake valve of turbine 2 failed, and 9 h were required to replace the actuators. Because turbines 1, 2, and 3 were stopped for this repair, the refrigeration power of He refrigerator was limited. As a result, the excitation in the superconducting system and the plasma experiment became discontinuous, and three days were needed for restoration.

The warm-up of the superconducting system started on August 4. During warm-up, increasing vibration was observed in one of the He compressors. However normal operation was restored within a stop time of only 30 min by switching to a redundant compressor. The 19th operational cycle completed successfully on August 25, with the total operating time of 5,761 h being the longest one in LHD's operating history.

B. Operational History and Availability of LHD

Fig. 5 summarizes the operational history of the LHD cryogenic system. The system's total operating time until the end of the 19th cycle was 84,073 h. The steady-state operating time in the superconducting state was 54,653 h; purification, cool-down and warm-up time was 29,420 h; and stop time that we have to stop the He compressors due to failures was 742.7 h.

Fig. 6 shows the availability in each operational cycle. The availability is calculated by Equation (1) using the mean time between failures (*MTBF*) and mean time to repair (*MTTR*). After early failures at the start of operation, the LHD cryogenic system showed high average availability of 99.1%.

$$Availability = MTBF/\left(MTBF + MTTR\right) \tag{1}$$

The number of system failures decreased over 20 years of operation. Table II list number of failure, total stop time and MTTR according to the failure cause. Control system failures occurred most frequently along with large influence compressor failure because of long MTTR. A total of 28 failures caused the cryogenic system to stop. However, the total down time was only 742.7 h.

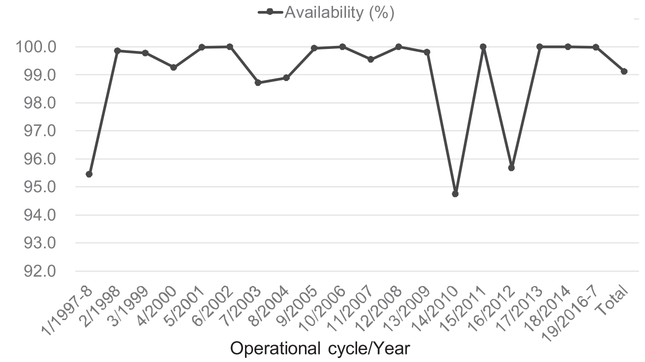

Fig. 6. Availability of the LHD cryogenic system.

TABLE II
FAILURE ANALYSES OF THE LHD CRYOGENIC SYSTEM

Cause of failure	Number of failures	Total stop time (h)	MTTR (h)
Control system	11	287.4	26.1
Compressors	6	268.7	44.8
Superconducting coils	1	169.0	169.0
Loss of electric power	5	10.0	2.0
Utility	4	7.5	1.9
Miss operation	1	0.1	0.1
Total	28	742.7	26.5

IV. CONCLUSION

The LHD suffered a fire, for which repair work started in November 2015 and completed at the end of July 2016. Then, the cooling power was reexamined through test operations in August 2016. Finally, the LHD restarted operation in January 2017, and its 19th operational cycle for the deuterium plasma experiment was successfully conducted up to August 2017. The degradation of the LHD cryogenic system has been minimized through appropriate maintenance, and its performance has been well maintained despite 20 years of operation. The LHD cryogenic system has operated reliably with high availability of 99.1%, and its total operating time from 1997 to 2017 was 84,073 h.

REFERENCES

[1] T. Mito *et al.*, "Design, development and operation of superconducting system for LHD," in *Proc. 19th Symp. Fusion Eng.*, 2002, pp. 144–151.

[2] T. Mito *et al.*, "Improvements of the LHD cryogenic system for further highly reliable operations," in *Proc. 24th Int. Cryogenic Eng. Conf./Int. Cryogenic Mater. Conf.*, 2013, pp. 449–452.

[3] T. Mito *et al.*, "Renewal of the control system and reliable long term operation of the LHD cryogenic system," *Phys. Procedia*, vol. 67, pp. 77–82, 2015, doi: 10.1016/j.phpro.2015.06.014.

[4] S. Imagawa *et al.*, "Effects of subcooling on lengths of propagating normal zones in the LHD helical coils," *IEEE Trans. Appl. Supercond.*, vol. 25, no. 3, Jun. 2015, Art. no. 4201805, doi: 10.1109/TASC.2014.2376994.

[5] T. Mito, "Long-term operational performance of the LHD cryogenic system," *TEION KOGAKU (J. Cryo. Super. Soc. Jpn.)*, vol. 50, no. 12, pp. 566–574, 2015.